Impact of switching of the electrical harvesting interface on microbial fuel cell losses

Armande Capitaine, Gaël Pillonnet, Thibaut Chailloux, Adrien Morel, Bruno Allard

Impact of switching of the electrical harvesting interface on microbial fuel cell losses

Armande Capitaine[1,2], Gael Pillonnet[1], Thibaut Chailloux[1], Adrien Morel[1] and Bruno Allard[2]
[1] Univ. Grenoble Alpes, CEA, LETI, DACLE, LGECA, F-38000 Grenoble, France
[2] Univ. de Lyon, INSA Lyon, Ampère, UMR CNRS 5005, F-69621 Villeurbanne, France

***Abstract*—Microbial fuel cells (MFCs) are sources harvesting energy from organic matters and showing great promise in powering environmental sensors. Because of the low power and voltage issues (100µW at 0.3V for 20 cm² electrodes), an electrical interface is required to extract the maximum power delivered by the MFC and boost the output voltage. However the switching operation of most converters induces a pulsed sinking current which may cause additional dynamic losses inside the MFC. Following a previous study on a flyback converter in discontinuous conduction mode, this paper analyzes the effect of switching of the converter on the MFC internal losses. A dynamic model of the MFC is deduced from an impedance spectroscopy characterization: it reveals a double RC behavior, one with a time constant of 10s of s, the other one of 100s of µs. Then in the frequency-domain, the MFC dynamic losses, induced by a previously optimized flyback, are calculated: they represent 50% of the maximum power that can be extracted from the MFC. Eventually in order to reduce these losses, we study the impact of three flyback parameters (primary inductance, duty cycle and decoupling capacitance). Adding a capacitance of 10 µF at the converter input, the MFC dynamic losses become negligible.**

Keywords*—microbial fuel cell; flyback converter; energy harvesting; dynamic electrical model; impedance spectroscopy

I. Introduction

Discovered in the last decades, microbial fuel cells (MFCs) are promising sources for scavenging energy from organic substrates (e.g. compost, sediment, wastewater…) by converting chemical energy into electricity thanks to catalysis properties of electro-active bacteria [1]. They can be seen as an attractive alternative to polluting batteries to power sensors in hardly reachable areas (e.g. seafloors). Regarding the low voltage and low power the MFCs generate (100 µW at 0.3 V for 20 cm² electrodes [2]), an electrical interface, i.e. a DC/DC converter, is required to extract the maximum power, P_{MPP}, from the MFC and boost the voltage to the level required by the sensor. However these converters, because of their inherent switching operation, impose a pulsed sinking current which may cause additional losses inside the MFC, on top of the well-known losses due to the DC current (static losses). These additional losses due to AC currents are called MFC dynamic losses. The paper follows a previous work [3, 4] where the MFC interface is a flyback converter in discontinuous conduction mode (DCM) extracting energy from a benthic MFC with 20 cm² electrodes and a maximum power of 90 µW. So far only the MFC static losses have been considered in literature. The paper studies the MFC additional dynamic losses induced by the switching operation of the flyback converter.

First a dynamic model of the MFC will be determined from experimental data obtained with electrochemical impedance spectroscopy (EIS) [5]. Then we will study the impact of the dynamic current imposed by the converter on the MFC dynamic losses. After developing a calculation method of the MFC dynamic losses, we will analyze the influence of three converter parameters (primary inductance, duty cycle, input capacitance) on these losses for minimization, i.e. avoid inefficient consumption of the organic substrate.

II. Electrical Modeling of MFC

A. Static behavior

A typical way to model the MFC static behavior is shown in Fig. 1. The polarization curve is comparable to a straight line corresponding to a Thevenin circuit. Our lab-scale MFC generates P_{MPP} = 90 µW at the maximum power point (MPP) and corresponds to an open-circuit voltage source V_{OC} of 0.6 V and a series resistance R_{DC} of 1 kΩ [2]. However this model does not reflect the dynamic behavior of the MFC when an AC stimuli is applied.

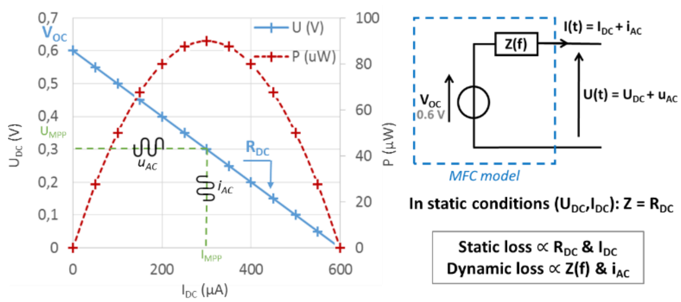

Fig. 1. Static characteristic of the MFC associated to the MFC electrical model

B. Dynamic characterization

The EIS method is adopted in order to to appreciate the MFC dynamic behavior at different DC operating point (U_{DC}, I_{DC}). This method consists in adding a sinusoidal perturbation u_{AC} with variable frequency f to the polarization voltage U_{DC} (as schematized in Fig. 1). The amplitude of u_{AC} is fixed to 50 mV so that the MFC can accurately be apprehended as a linear system. The resulting current, expressed as the sum of the static current I_{DC} and a sinusoidal perturbation i_{AC}, is then measured. From these measurements, we can deduce an MFC equivalent dynamic impedance Z(f) at different frequency f for a specific DC point (U_{DC}, I_{DC}). Its amplitude |Z| and phase φ, when working at MPP (U_{DC} = 0.3V), are represented in Fig. 2. Similar AC characteristic is obtained for other polarization voltages. Weassume the MFC dynamic behavior is independent of the polarization point. Moreover the frequency range is large since some physical aspects characterized at low frequency (e.g. mHz) may have a significant impact even when using a kHz switching frequency converter.

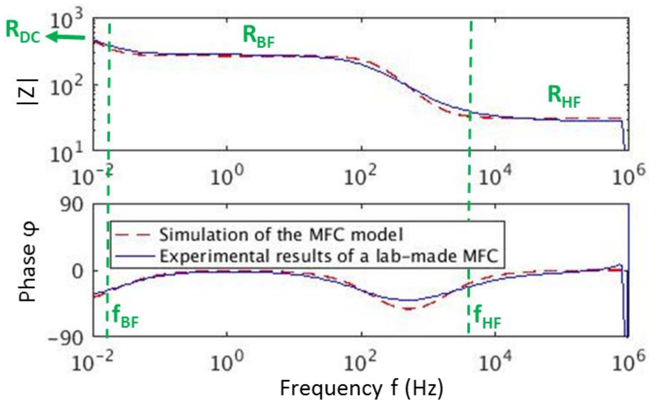

Fig. 2. Amplitude and phase of the MFC dynamic impedance obtained experimentally with the impedance spectroscopy method (blue solid line) and of the deduced dynamic model of the MFC (red dashed line).

C. Dynamic electrical model

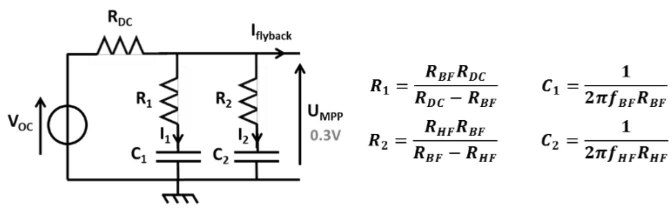

Fig. 3. Dynamic model of the MFC

The dynamic electrical circuit deduced from the previous characterization is represented in Fig. 3. To the static model is added two parallel RC branches, one (R_1C_1) being associated to the low cut-off frequency f_{BF}, the other (R_2C_2) to the higher one f_{HF} (Fig. 2). The circuit components are calculated using equations in Fig. 3 in which {R_{BF}, R_{HF}, f_{BF}, f_{HF}} are evaluated from AC measurements (Fig. 2). R_{DC} is not readable in Fig. 2 as extended AC measurements at lower frequencies is very time consuming. R_{DC} is thus deduced from a previous static characterization (Fig. 1). The results are listed in Table I..It shows an accurate fit with the experimental data (Fig. 2).

TABLE I. VALUES OF THE DYNAMIC MODEL COMPONENTS

R_{DC}	R_1	C_1	R_2	C_2
1 kΩ	347 Ω	30 mF	35 Ω	3 µF

The first branch R_1C_1 has a time constant of the order of 10s of seconds and can be associated to the transport mechanisms of the organic matter to the electrodes [6]. Whereas the second branch R_2C_2, having a time constant of the order of 100s of microseconds may be due to the double layer electrical behavior at the electrodes' surface [6]. Therefore the MFC presents two dynamic resistances R_1 and R_2 that may engender additional intrinsic losses.

III. Influence of the Harvesting Interface on the MFC Dynamic Losses

A. Harvesting interface

Using the previous work presented in [3], the flyback in DCM is chosen as an harvesting interface mainly for its isolation capability. As explained in [3], to work at the DC-MPP and extract the maximum DC energy from the MFC, the flyback input impedance R_{IN} has to meet the following constraints:

$$R_{IN} = \frac{2L_1 f_{sw}}{D^2} = R_{DC} \quad (1)$$

L_1 is the primary inductance, D the duty cycle and f_{sw} the switching frequency of the flyback. This means the three parameters {L_1, D, f_{sw}} are linked. In [4] it was chosen to work with a coreless transformer to avoid converter losses due to saturation and hysteresis and thus maximize the converter efficiency. The same experimental set-up {L_1, D, f_{sw}} = {583 µH, 0.07, 4.23 kHz} will be used in the following study to evaluate the additionnal AC losses due to R_1 and R_2.

B. Calculation of the MFC dynamic losses

Transient simulations may be very time consuming regarding the 10s of second time constant at stake in the MFC dynamic model compared to kHz flyback switching operation and so the time needed to reach steady-state operation. An analytical frequency approach based on the Fourier decomposition is thus preferred. For the sake of simplification, the flyback input current, called $I_{flyback}$ in Fig. 4, is considered of constant at the flyback input and independent of MFC energy production. In frequency domain, we calculate the Fourier series of currents I_1 and I_2 in Fig. 3 using the respective transfer functions regarding $I_{flyback}$ and the Fourier series of $I_{flyback}$. Again in the time-domain, the losses P_1 and P_2 induced respectively by the branch R_1C_1 and R_2C_2 are deduced. The method is summarized for P_1 in Fig. 4.

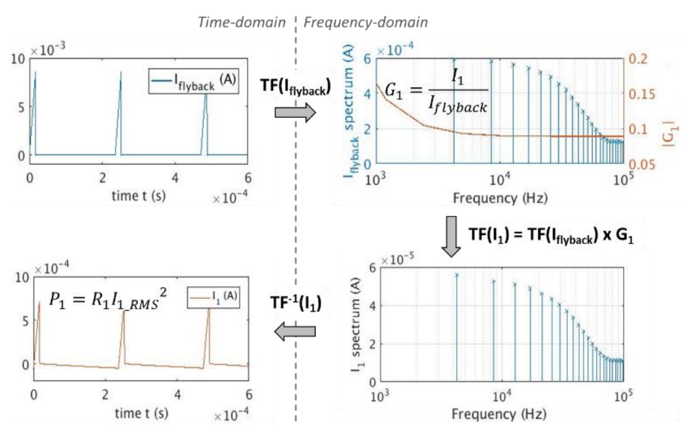

Fig. 4. Method of the dynamic losses calculation, example of P_1 calculation

C. Results

Following this calculation process, in the chosen conditions {L_1, D, f_{sw}} = {583 µH, 0.07, 4.23 kHz}, P_1 is equal to 4.4 µW and P_2 to 42.9 µW, representing respectively 5% and 48% of the extracted DC power P_{MPP} (equal to 90 µW). Therefore the dynamic part of the MFC undergoes non-negligible losses compared to the 90 µW corresponding to the DC losses due R_{DC}.

This means a power equivalent to 53% of the one usefully delivered to the converter is lost inside the MFC, contributing to a useless depletion of the organic matter resources. In order to reduce these losses, we will vary different flyback parameters, e.g. L_1 and D, to change the frequency spectrum of the currents I_1 and I_2 and thus the energy dissipation in respectively in R_1 and R_2.

Influence of L_1: fixing D to 0.07, P_1 and P_2 are calculated for L_1 varying from 2 µF to 200 mF. In order to respect (1) and work at the DC-MPP, f_{sw} is constantly adapted (from 1.23 MHz to 12.3 Hz). The results are shown in Fig. 5. When increasing L_1, i.e. decreasing f_{sw}, I_1 increases ($|G_1|$ increases in the lower frequencies, Fig. 4) while I_2 decreases. Regarding the high value of R_1 compared to R_2, the increase in P_1 is more significant than the decrease in P_2, hence the total dynamic losses explode, especially for $L_1 > 100$ mH. For lower values, L_1 variations have no impact on the dynamic losses which remain equal to 52.6% of P_{MPP}. Therefore considering our previous working conditions ($L_1 = 583$ µH), no minimization of the dynamic losses can be made by varying L_1.

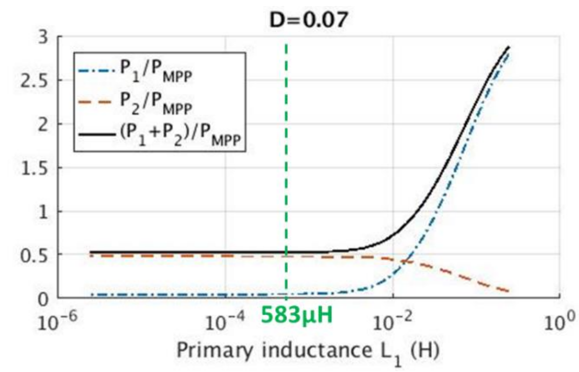

Fig. 5. Influence of L_1 choice on the MFC dynamic losses (D=0.07)

Influence of D: L_1 is fixed to 583 µH and D varies from 0 to 1 while adapting f_{sw} according to (1) as it was done in the previous case. The results are shown in Fig. 6. When decreasing D, i.e. decreasing f_{sw}, the dynamic losses increase exponentially. These losses are particularly important when working with D lower than 0.2. Then working with a D higher than 0.5, i.e. f_{sw} higher than 214 kHz, ensures negligible dynamic losses. However [3] has shown that such an increase in f_{sw} causes critical switching losses inside the flyback and thus drastically reduces its conversion efficiency. Therefore another way to reduce P_1 and P_2 without impacting on the conversion efficiency is needed.

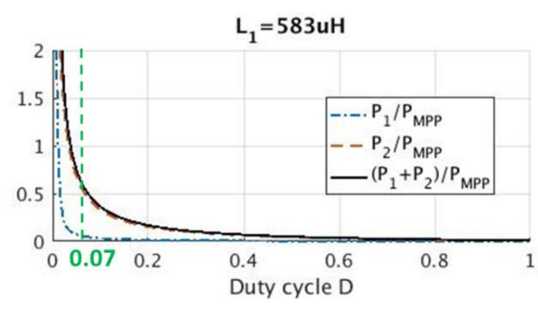

Fig. 6. Influence of D choice on the MFC dynamic losses (L_1=583µH)

Influence of C_{IN}: using the initial parameters given in section III.A, a capacitance is added at the input of the flyback converter. The results are displayed in Fig. 7. We observe that the inclusion of this capacitance decreases the MFC dynamic losses. This decrease becomes significant for C_{IN} larger than few µF for which the dynamic losses represent less than 1% of the extracted power P_{MPP}. With C_{IN} = 10 µF (which represents a negligible extra surface on a PCB), these losses are equal to 0.1% of P_{MPP} and may be neglected. Indeed all the AC current is flows in C_{IN}, causing no loss as ESR is neglected.

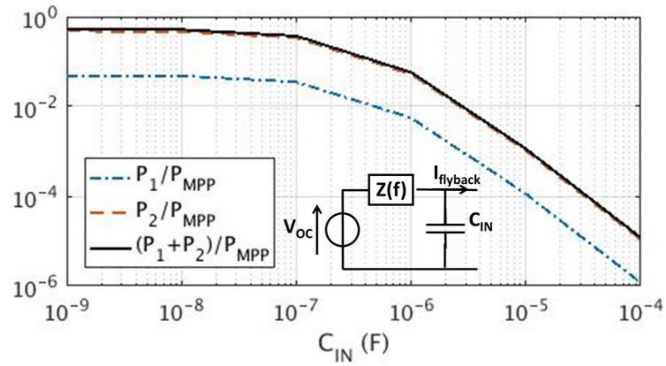

Fig. 7. Influence of a capacitance C_{IN} at the input of the flyback on the MFC dynamic losses ({L1, D, fsw} = {583 µH, 0.07, 4.23 kHz})

IV. CONCLUSION

The paper analyzes the influence of the flyback converter in DCM on the intrinsic losses of an MFC. Because of the switching behavior, the converter imposes dynamic currents to the MFC which may induce dynamic losses inside the MFC. First a dynamic model composed of two parallel RC branches associated to time constants of the order of 100s of µs and 10s of s was deduced from measurements obtained with EIS. Second we analyzed the influence of the flyback design (always working at MPP) on the losses induced by these two dynamic branches. Varying L_1 offers no possible optimization, while increasing D may significantly reduce the dynamic losses. However increasing D means increasing f which drastically reduces the flyback efficiency. Eventually we show that inserting a decoupling capacitance larger than 10 µF at the input of the converter reduces the MFC dynamic losses from 52.6% to 0.1% of the extracted power P_{MPP}.

REFERENCES

[1] B.E. Logan et al., Microbial fuel cells: methodology and technology, Environ. Sci. Technol., 40 (2006) 5181-5192.

[2] T. Chailloux et al., Autonomous sensor node powered by cm-scale benthic microbial fuel cell and low-cost and off-the-shelf components, Energy Harvesting and Systems, 3 (2016) 205-212.

[3] A. Capitaine et al., Loss analysis of flyback in discontinuous conduction mode for sub-mW harvesting systems, IEEE Proceedings of new Circuits and Systems Conference (NEWCAS), 2016.

[4] Y. Wanderoild et al., 100 µW coreless flyback converter for microbial fuel cells energy harvesting, New generation of circuits and systems (NGCAS), 2017, in press.

[5] X. Z. Yuan et al., Electrochemical impedance spectroscopy in PEM fuel cells, Springer, 2010

[6] A. Dhirde et al., Equivalent electric circuit modeling and performance analysis of a PEM fuel cell stack using impedance spectroscopy, IEEE Transactions on energy conversion, 25 (2010) 778-786.